Virology xxx (xxxx) xxx–xxx

Contents lists available at ScienceDirect

Virology

journal homepage: www.elsevier.com/locate/virology

Respiratory disease in ball pythons (*Python regius*) experimentally infected with ball python nidovirus

Laura L. Hoon-Hanks[a,*], Marylee L. Layton[a], Robert J. Ossiboff[b,1], John S.L. Parker[c], Edward J. Dubovi[b], Mark D. Stenglein[a,**]

[a] Department of Microbiology, Immunology, and Pathology, College of Veterinary Medicine and Biomedical Sciences, Colorado State University, Fort Collins, CO, USA
[b] Department of Population Medicine and Diagnostic Sciences, College of Veterinary Medicine, Cornell University, Ithaca, NY, USA
[c] Baker Institute for Animal Health, College of Veterinary Medicine, Cornell University, Ithaca, NY, USA

ARTICLE INFO

Keywords:
Ball python
Nidovirus
Experimental infection
Respiratory disease
Pneumonia
Torovirinae
Barnivirus
Koch's postulates

ABSTRACT

Circumstantial evidence has linked a new group of nidoviruses with respiratory disease in pythons, lizards, and cattle. We conducted experimental infections in ball pythons (*Python regius*) to test the hypothesis that ball python nidovirus (BPNV) infection results in respiratory disease. Three ball pythons were inoculated orally and intratracheally with cell culture isolated BPNV and two were sham inoculated. Antemortem choanal, oroesophageal, and cloacal swabs and postmortem tissues of infected snakes were positive for viral RNA, protein, and infectious virus by qRT-PCR, immunohistochemistry, western blot and virus isolation. Clinical signs included oral mucosal reddening, abundant mucus secretions, open-mouthed breathing, and anorexia. Histologic lesions included chronic-active mucinous rhinitis, stomatitis, tracheitis, esophagitis and proliferative interstitial pneumonia. Control snakes remained negative and free of clinical signs throughout the experiment. Our findings establish a causal relationship between nidovirus infection and respiratory disease in ball pythons and shed light on disease progression and transmission.

1. Importance

Over the past several years, nidovirus infection has been circumstantially linked to fatal respiratory disease in multiple python species, but a causal relationship has not been definitively established. Through experimental infections, our study fulfills Koch's postulates and confirms ball python nidovirus as a primary respiratory pathogen in this species. Our findings will provide veterinarians valuable information for the diagnosis and management of this disease and lay the groundwork for continued scientific investigation of this sometimes fatal disease. Python nidoviruses are members of a growing group of viruses that have been associated with severe respiratory disease, including bovine nidovirus and shingleback lizard nidovirus. The establishment of BPNV as a primary pathogen in pythons is an important step in understanding the pathogenic potential of this emerging group of viruses.

2. Introduction

The nidoviruses (order *Nidovirales*) are a large and diverse group of viruses that includes notable human and veterinary pathogens (De Groot et al., 2012; Graham et al., 2013; Lauber et al., 2012; Masters and Perlman, 2013; Snijder et al., 2013; Snijder and Kikkert, 2013). The discovery of a group of related nidoviruses in snakes, lizards, cattle, and nematodes has recently expanded the order (Bodewes et al., 2014; Dervas et al., 2017; Marschang and Kolesnik, 2017; O'Dea et al., 2016; Shi et al., 2016; Stenglein et al., 2014; Tokarz et al., 2015; Uccellini et al., 2014). These novel nidoviruses cluster most closely with viruses in the subfamily *Torovirinae* within the *Coronaviridae* family of the *Nidovirales* order, and form a distinct clade from viruses in the *Bafinivirus* and *Torovirus* genuses, which infect ray-finned fish and mammals, respectively. Based on phylogenetic analysis, it has been proposed that the reptile nidoviruses be classified within a distinct genus named *Barnivirus*, and that *Torovirinae* be classified as its own family due to the growing evidence of the paraphyly of *Coronaviridae*, though these viruses have not yet been formally classified (Adams et al., 2017; Batts et al., 2012; Gonzalez et al., 2003; Nga et al., 2011; Stenglein et al., 2014). Toroviruses share similar tissue tropisms of the gastrointestinal (GI) and respiratory epithelium, ultrastructural features, and genome

* Correspondence to: Colorado State University, 200 W Lake St. 2025 Campus Delivery, Fort Collins, CO 80523, USA.
** Co-corresponding author.
E-mail addresses: laura.hoon-hanks@colostate.edu (L.L. Hoon-Hanks), mark.stenglein@colostate.edu (M.D. Stenglein).
[1] Current address: Department of Comparative, Diagnostic, and Population Medicine, College of Veterinary Medicine, University of Florida, Gainesville, FL, USA.

https://doi.org/10.1016/j.virol.2017.12.008
Received 29 September 2017; Received in revised form 1 December 2017; Accepted 11 December 2017

organization (Batts et al., 2012; Pradesh et al., 2014; Schutze et al., 2006), and represent a group of emerging pathogens of unknown, and possibly underestimated, significance in veterinary and human medicine.

The snake-associated nidoviruses were first discovered in ball pythons (*Python regius*) and Indian rock pythons (*P. molurus*) with severe respiratory disease that had tested negative for known snake respiratory pathogens (Bodewes et al., 2014; Stenglein et al., 2014; Uccellini et al., 2014). Postmortem findings in sick pythons included stomatitis, sinusitis, pharyngitis, tracheitis, esophagitis, and proliferative pneumonia with significant mucus secretion in affected tissues; secondary bacterial infections were also noted within the respiratory tract or systemically in some snakes. In 2017, similar findings were detected in green tree pythons (*Morelia* [*M.*] *viridis*) infected by a related nidovirus (*Morelia viridis* nidovirus) (Dervas et al., 2017). Additionally, nidoviruses have been detected in antemortem oral swabs (or rarely blood) from a Burmese python (*P. bivittatus*), ball pythons, Indian rock pythons, green tree pythons, a carpet python (*M. spilota*), and boa constrictors (*Boa constrictor*) with or without documented respiratory signs (Marschang and Kolesnik, 2017). Related nidoviruses associated with respiratory disease in wild shingleback lizards and cattle have also been recently described (O'Dea et al., 2016; Tokarz et al., 2015).

Reports of nidovirus in multiple python species are highly suggestive of, but do not definitively establish, a causal relationship between viral infection and respiratory disease. This study sought to fulfill Koch's postulates through experimental infections of ball pythons with ball python nidovirus (BPNV). The goal was to conclusively establish a causative relationship between infection and respiratory disease as well as further characterize the clinical course of disease, describe useful diagnostic techniques, and to investigate possible routes of transmission.

3. Materials and methods

3.1. Generation of a diamond python cell line

A non-immortalized cell line was generated from heart tissue collected from a diamond python (*Morelia spilota*). Multiple ~ 2 mm cubes of myocardium were collected from a diamond python directly following humane barbiturate overdose euthanasia for chronic vertebral disease. Tissues were collected within 2 h of euthanasia and placed in 1.5 ml, ice-cold, sterile phosphate buffered saline (PBS) in 2 ml microcentrifuge tubes for transport to the laboratory. Tissue samples were individually transferred to a 6-well cell culture plate (Corning), washed three times with ice cold PBS, and manually minced with a sterile scalpel blade in 1.5 ml PBS with 0.25% trypsin (Gibco) and 1 mM ethylenediaminetetraacetic acid (EDTA). Samples were incubated at 37 °C with gentle agitation every 20 min (m) for a total of 60 m. Following incubation, 0.5 ml of the digested product was added per well of a 12-well cell culture plate (Corning) along with 2 ml of complete cell growth medium [Minimum Essential Medium with Earle's Balanced Salts, L-Glutamine, and Nonessential Amino Acids (MEM/EBSS; Hyclone); 10% irradiated fetal bovine serum (FBS; HyClone); 100 U penicillin; 100 µg streptomycin; 0.25 µg amphotericin B (Cellgro); and 50 µg gentamicin (Cellgro)] and placed at 30 °C in a humidified 5% CO_2 atmosphere. Wells were monitored regularly for evidence of cell adherence and replication. Partial (~ 50%) medium changes were performed weekly. When cell monolayers reached ~ 70% confluence, monolayers were washed twice with room temperature sterile PBS, 1 ml enzyme free cell dissociation buffer (Gibco) was added to each well, and the samples were incubated for 5 m at 30 °C. Cell monolayers were disrupted by gently pipetting samples up and down, and the cell/dissociation buffer mixture was transferred to a 60 mm tissue culture dish (Corning) with 7 ml of complete cell growth medium and returned to a 30 °C, humidified, 5% CO_2 atmosphere. The cells were monitored regularly for evidence of cellular replication with weekly, partial (~ 50%) medium changes. At ~ 70% confluence, monolayers were passed using 0.25% trypsin first into T25, and then into T75 tissue culture flasks (Corning). At 100% confluence, T75 flasks were trypsinized, washed in complete cell growth medium, and resuspended in 1 ml of complete cell growth medium with 20% irradiated FBS and 10% DMSO for storage in liquid nitrogen in 1.2 ml cryovials (Corning).

3.2. Isolation of BPNV

Oral swabs were collected from a ball python with upper respiratory disease that was part of a colony with a documented history of BPNV infections (Uccellini et al., 2014). Swabs were placed in 1.5 ml of viral transport medium (MEM/EBSS, 0.5% bovine serum albumin, 200 U penicillin, 200 µg streptomycin, 0.25 µg fungizone, and 10 µg ciprofloxacin; Gibco) prior to inoculation on diamond python heart (DPHt) cells. Briefly, 1 ml of the swab extracts were added to DPHt cells in T25 culture flasks. After a 3 h incubation at 30 °C, monolayers were rinsed and cell growth medium added (MEM/EBSS, 10% irradiated FBS, 200 U penicillin, 200 µg streptomycin, 0.25 µg fungizone, and 10 µg ciprofloxacin; Gibco). Cultures were maintained at 30 °C and monitored daily for cytopathic effects. At 7 days post inoculation cells were frozen at − 70 °C, thawed, and were re-inoculated onto new DPHt monolayers. The study challenge virus (deemed BPNV-148) was a passage 2 preparation.

3.3. Plaque assay

DPHt cells were incubated in complete cell medium [MEM/EBSS (HyClone), 10% irradiated FBS (HyClone), 10% Nu-Serum1 (Corning), and 2x penicillin-streptomycin solution (HyClone)] in a 6-well CELLSTAR cell culture plate (Greiner Bio-one) at 30 °C in 5% CO_2 until 90% confluence was attained. BPNV-148 stock was diluted in serum-free MEM/EBSS to generate 5 dilutions of 1×10^{-2} through 1×10^{-6}. For cell inoculation, all medium was removed and 900 µl of each dilution was placed on the cells, with serum-free MEM/EBSS added to the last well as a negative control. Cells were incubated at 30 °C in 5% CO_2 for 1 h, after which the infected medium was removed and an agarose overlay was placed [complete cell medium with 0.8% UltraPure LMP Agarose (Invitrogen)]. Assays were incubated at 30 °C in 5% CO_2 for 6 days, at which time 1 ml of 4% paraformaldehyde (EM grade; Electron Microscopy Sciences) in DPBS (Corning) was added to each well and incubated for an additional hour. The agarose overlay was removed, cells were rinsed with DPBS, and an additional 1 ml of paraformaldehyde mixture was added. Cells were placed at 4 °C overnight. The formaldehyde was removed, cells were rinsed with sterile water, and 100 µl of crystal violet (0.5% crystal violet in 25% methanol and 75% sterile water) was added and incubated for 10 min at room temperature. Crystal violet was rinsed off with sterile water, assays were dried, and plaques were counted. Plaque assays were also performed using samples collected during experimental infection studies; the same protocol was utilized.

3.4. Experimental infection

Five captive-bred ball pythons (BP A-E; 4 males and one undetermined sex) were acquired, each approximately 6 weeks old and varying in size from 77 to 106 g. All pythons were housed and treated according to the IACUC protocol (15–6063A) and Colorado State University Laboratory Animal Resources standards. Infected snakes were housed in a cubicle with separate HEPA-filtered air supply from control snakes and all snakes were housed in separate cages without direct contact. Uninfected snakes were always handled prior to infected snakes to prevent fomite transmission. Physical exams were performed and all snakes were deemed clinically healthy at the time of acquisition. Pre-infection choanal (CHS), oroesophageal (OES), and cloacal swabs (CLS) were collected and tested by qRT-PCR (see below) for BPNV. One

week after arrival, three snakes were inoculated with BPNV infected DPHt cell culture supernatant discussed above (BP-A, B, and C) and two were sham inoculated (BP-D and E). Inoculation was performed both orally (200 µl) and intratracheally (100 µl) for each snake with 1.1 × 10^5 PFU in 300 µl for the infected snakes and a similar volume of uninfected cell culture medium for the control snakes. Snakes were monitored daily, weights were taken weekly, and CHS, OES, and CLS were collected weekly from all snakes using PurFlock Ultra sterile flocked 6″ plastic-handle swabs (Puritan Diagnostics). Swabs were placed in 2 ml Bacto brain-heart infusion medium (Becton, Dickinson and Company), incubated at room temperature (RT) for approximately 30 min, vortexed, and then stored at − 80 °C. BP-C was euthanized at 5 weeks post infection (PI) as a demonstration of early infection. BP-A was euthanized at 10 weeks PI and BP-B at 12 weeks PI based on clinical signs and established euthanasia criteria. BP-D and E were euthanized at 12 weeks to end the study. Final CHS, OES, and CLS and culture swabs of the oral cavity (BBL CultureSwab plus Amies gel without charcoal; Becton, Dickinson and Company) were collected at the time of euthanasia. Sections of the glottis, nasal and oral cavity, cranial, middle, and caudal trachea and esophagus, lungs, heart, liver, kidneys, gallbladder, spleen, pancreas, stomach, small intestine, colon, feces, blood, urates, gonads, head and vertebrae with brain and spinal cord were saved fresh and/or placed in 10% neutral buffered formalin.

3.5. RNA extraction

RNA from swabs and fresh-frozen tissues (lung, cranial trachea/esophagus, liver, kidney, heart, stomach, small intestine, colon, feces, urates) was extracted using a combination of TRIzol (tissue; Ambion Life Technologies) or TRIzol LS (swabs in BHI; Ambion Life Technologies) with RNA clean and concentrator columns (CC-5; Zymo Research). Approximately 100 mg of tissue was added to 1 ml of TRIzol and 250 µl of BHI swab medium was added to 750 µl of TRIzol LS and incubated at room temperature (RT) for 5 min. Tissue samples were macerated using a single sterile metal BB shaken in a TissueLyzer (Qiagen) at 30 Hz for 3 min. Then, 200 µl of chloroform (Sigma-Aldrich) was added, shaken for 15 s by hand, and incubated at RT for 2 min. Samples were spun at 12,000 RPM for 10 min at RT. The aqueous phase was removed (approximately 450 µl) and was added to a mixture of 450 µl of RNA binding buffer (CC-5; Zymo Research) and 450 µl of 100% ethanol (EtOH). This was added to an RNA clean and concentrator column (CC-5; Zymo Research). The interphase and organic phase were discarded. The RNA column was washed with 400 µl RNA wash buffer and then incubated with 6 U DNase enzyme (NEB), 1x DNase buffer (NEB), and RNA wash buffer for 15 min. The column was spun to remove DNase mixture and then washed with 400 µl RNA prep buffer. An additional wash with 800 µl RNA wash buffer was performed, the column was dried with a 1 min high-speed spin, and then RNA samples were eluted in 30 µl of RNase-free water.

3.6. Viral RNA detection

RNA extracted from swabs and fresh-frozen tissues was reverse transcribed into cDNA as follows. Five microliters of RNA were added to 200 pmol of a random pentadecamer oligonucleotide (MDS-911; Table 1) and incubated for 5 min at 37 °C; a water template control was also used. Reverse transcription reaction mixture containing 1x SuperScript III FS reaction buffer (Invitrogen), 5 mM dithiothreitol (Invitrogen), 1 mM each deoxynucleoside triphosphates (dNTPs), and 100 U SuperScript III reverse transcriptase enzyme (Invitrogen) was added to the RNA-oligomer mix (12 µl total reaction volume) and incubated for 30 min at 42 °C, then 30 min at 50 °C, then 15 min at 70 °C. Quantitative reverse transcription polymerase chain reaction (qRT-PCR) was performed using 1x HOT FIREPol DNA Polymerase (Solis BioDyne), 3 µM of each degenerate nidovirus primer (MDS-918 and MDS-919; Table 1), and 5 µl of diluted (1:10) cDNA in a 30 µl reaction. Reaction mixtures were placed in a TempPlate semi-skirted 96-well PCR plate and were run in a Roche LightCycler 480 II with the following cycle parameters: 95 °C for 15 min; 95 °C for 10 s, 60 °C for 12 s, and 72 °C for 12 s with 40 cycles; and a melting curve. All samples were run in duplicate, Ct values were averaged and standard deviations were calculated. The PCR reaction efficiency for each primer-pair was measured using a dilution series of positive samples (BP-B terminal OES for nidovirus primers and BP-B trachea/esophagus for GAPDH primers); the dilution series samples were run in duplicate. Relative viral RNA for all CHS, OES, and CLS samples was determined by comparison of each sample Ct to the sample with the highest Ct (lowest viral RNA) at the first collection time point following inoculation (BP-B OES at week 1 PI). Relative viral RNA from tissues was determined by normalization to snake GAPDH within each sample (same qRT-PCR conditions with MDS-921and MDS-923 primers; Table 1).

3.7. Antibody development

The predicted amino acid (aa) sequence for the ball python nidovirus 1 nucleocapsid protein (152 aa protein; GenBank: AIJ50569.1) and nidovirus nucleocapsid protein sequences isolated from green tree pythons (unpublished data) were used by our lab to identify a relatively conserved peptide sequence with predicted high immunogenicity and epitope exposure. The peptide (aa 136–152 of the N protein of a green tree python nidoviral isolate: Cys-RAFIPLKHEGAETEEEV) was submitted to Pacific Immunology (Ramona, CA) for synthesis and polyclonal anti-nidoviral nucleocapsid antisera (NdvNcAb) was developed in two rabbits.

3.8. Histopathology/immunohistochemistry

Formalin-fixed tissue was paraffin-embedded and 5 µm sections were stained by hematoxylin and eosin (H&E), Gram, periodic acid-Schiff (PAS), and Ziehl-Neelsen acid fast for light microscopy (performed by Colorado State University Veterinary Diagnostic Laboratory; CSUVDL). Immunohistochemistry was also performed by CSUVDL using the Bond Polymer Redefine Red Detection kit (Leica) and a 10 min incubation with Epitope Retrieval Solution 1 (Leica). NdvNcAb (0.32 µg/ml) was used as the primary antibody and the slides were counter stained with hematoxylin. Lung tissue from a green tree python that was nidovirus positive (PCR and virus isolation) and that died of respiratory disease was used as a positive control (data not shown).

Table 1
Primers. List of primers used during qRT-PCR for detection of BPNV or GAPDH and used for sequencing library generation. Forward (F); Reverse (R); N/A (not applicable).

Primer name	Target	Sequence (5′-3′)	Direction (F/R)	Reference
MDS-143	Sequencing library adaptors	CAAGCAGAAGACGGCATACG	F	(Runckel et al., 2011)
MDS-445		AATGATACGGCGACCACCGA	R	
MDS-911	Random	NNNNNNNNNNNNNN	–	N/A
MDS-918	ORF1b python nidovirus	CAYAACATCGACATCGCACT	F	–
MDS-919		TCGATGAAGATYTCGGTGTT	R	
MDS-921	Python GAPDH gene	AATATCTGCCCCATCAGCTG	R	(Stenglein et al., 2017)
MDS-923		GTTTTCCAAGAGCGTGATCC	F	

3.9. Virus isolation and immunofluorescence

Oroesophageal swabs collected at the time of euthanasia from all infected and uninfected snakes were filtered (Merck Millipore UltraFree-MC 0.22 μm centrifugal filters) and 40 μl was inoculated onto DPHt cells at 80% confluence in 35 mm diameter glass-bottom plates (MatTek corporation). Cells were maintained in 2 ml of complete cell medium and incubated at 30 °C with 5% CO_2; medium was refreshed every other day. Cells infected with BP-A OES were formalin-fixed as previously described at 1, 12, 24, 48, 96, 144, and 192 h PI; all other OES-infected cells (BP-B, C, D, and E) were formalin-fixed at 4 days PI. Approximately 50 mg of lung or feces from infected and uninfected pythons was homogenized in 500 μl of DPBS, clarified, and then filtered (0.22 μm). Infection of cell culture was as previously described. Lung-infected cells were formalin-fixed at 10 days PI and fecal-infected cells at 3 days PI.

Fixed cells were washed 3 times with 1 ml of PBS. Cells were permeabilized in 0.1% Triton X-100 (reagent grade; Amresco) in PBS for 5 min. Washes were repeated and then cells were incubated in blocking buffer (1% bovine serum albumin (Fisher Scientific) in PBS) for 1 h. A 1:2000 dilution of NdvNcAb rabbit serum (primary antibody) was added to the blocking buffer and incubated for an additional hour. Wash steps were repeated and then new blocking buffer with 5 μg/ml of secondary antibody (Alexa Fluor 488 goat anti-rabbit IgG antibodies; A11008 Life Technologies) was added and incubated for 1 h. Wash steps were repeated and then cells were stained with Hoechst 33342 (1 μg/ml final concentration; Life Technologies) to stain DNA. Cells were imaged on an Olympus IX81 motorized inverted system confocal microscope with FluoView 4.2 software. Images were processed in Adobe Photoshop CC (2017) and both infected and uninfected were processed equally.

3.10. Western blot

DPHt cells inoculated with OES from all infected and uninfected snakes, as previously described, as well as a sham inoculated control (BHI only) were harvested at 4 days PI. Cells were lysed using equal volumes of sample and SDS-based tissue lysis buffer (40 mM TrisCl pH 7.6, 120 mM NaCl, 0.5% Triton X-100, 0.3% SDS, Roche complete protease inhibitor cocktail tablet), mixed for 30 min at 4 °C, and clarified by centrifugation at 4 °C for 10 min at 10,000 rpm. Twelve microliters of sample or 4 μl of ladder with 8 μl of PBS (precision plus protein western C; BioRad) were combined with 1x NuPage LDS sample buffer (Life Technologies) and separated using a 4–12% polyacrylamide gel (Invitrogen). Protein was transferred to a nitrocellulose membrane using a Trans-Blot turbo (low molecular weight protein transfer; Bio-Rad). A 1 h incubation of the membrane in blocking buffer [1x PBS, 0.05% Tween20, 1% Carnation nonfat dry milk, and 1:1000 Kathon CG/ICP preservative (Dow Chemical)] was followed by a 1 h incubation with 1.6 μg/ml NdvNcAb in blocking buffer. The membrane was washed (1x PBS and 0.05% Tween20) 3 times for 5 min each followed by a 1 h incubation with a 1:50,000 dilution of goat anti-rabbit IgG antibody conjugated to horseradish peroxidase (HrP; Pierce 31460 Invitrogen) and 1:4000 dilution of streptactin-HrP (ladder) in blocking buffer. A second wash was performed and the blot was developed using a 5 min incubation with clarity western ECL substrate (BioRad). Imaging was via chemiluminescence for 60 s (BioRad Gel Doc).

3.11. Metagenomic sequencing

Shotgun libraries were generated from total RNA extracted from BP-A, B, C, D, and E lung and cranial trachea/esophagus and BPNV-148 inoculum. Library preparation was as follows: Ten microliters of undiluted cDNA (see polymerase chain reaction for cDNA preparation) was treated with 1 U RNase H (NEB) diluted in 5 μl 1x SuperScript III FS reaction buffer and 160 pmol MDS-911 to degrade RNA templates. Samples were incubated at 37 °C for 20 min followed by 94 °C for 2 min. Then, single-stranded cDNA was converted to double-stranded DNA by adding 2.5 U Klenow DNA polymerase (3′ to 5′ exo- NEB) in 5 μl 1x SuperScript III FS reaction buffer and 2 mM each dNTPs and incubated at 37 °C for 15 min. DNA was purified using SPRI beads at a 1.4:1 bead/DNA volume ratio. DNA was eluted in 20 μl molecular grade water (Sigma-Aldrich). The dsDNA concentration from each sample was measured fluorometrically and 10 ng was used as a template in 6.5 μl of 1x Tagment DNA buffer and 0.5 μl Nextera Tagment DNA enzyme (Illumina). The mixture was incubated at 55 °C for 10 min and then placed directly on ice. Tagmented DNA was cleaned with SPRI beads and used as a template (5.8 μl) in the addition of full-length adaptors with unique bar-code combinations by PCR. The 25 μl PCR reaction contained 1x Kapa real-time library amplification master mix (Kapa Biosystems), 0.33 μM (each) MDS-143 and MDS-445 primers (Table 1), and 0.020 μM each of adaptor 1 and 2 bar-coded primers (Stenglein et al., 2015). Thermocycling conditions in consecutive order were 72 °C for 3 min, 98 °C for 30 s, and 8 cycles of 98 °C for 10 s, 63 °C for 30 s, and 72 °C for 3 min. Relative concentrations of libraries were measured in qRT-PCR reactions containing 1x qRT-PCR master mix [10 mM Tris-HCl pH 8.6, 50 mM KCl, 1.5 mM $MgCl_2$, 0.2 mM of each dNTP, 5% glycerol, 0.08% NP-40, 0.05% Tween-20, 1x Sybr green (Life Technologies) and 0.5 U Taq polymerase] and 0.5 μM MDS-143 and MDS-445 primers. Equivalent amounts of DNA from each sample were pooled and then cleaned using SPRI beads. The pooled libraries were run on a 2% agarose gel and size selected (400–500 nucleotides) by gel extraction with a gel DNA recovery kit (Zymo Research) according to the manufacturer's protocol. Size-selected pooled libraries were amplified once more in a PCR mixture containing 1x Kapa real-time library amplification mix, 500 pmol of MDS-143 and -445 each, and 5 μl of library template in a 50 μl total reaction volume. This PCR also included single reactions of 4 separate fluorometric standards (Kapa). Thermocycler conditions were 98 °C for 45 s and 14 cycles of 98 °C for 10 s, 63 °C for 30 s, and 72 °C for 2 min, which was the cycle at which the sample curve passed standard 1. DNA was purified using SPRI beads as previously described. Library quantification was performed with the Illumina library quantification kit (Kapa Biosystems) according to the manufacturer's protocol. Paired-end 2 × 150 sequencing was performed on an Illumina NextSeq. 500 instrument with a NextSeq. 500/550 Mid Output Kit v2 (300 cycles).

3.12. Sequence analysis

Sequences were trimmed using Cutadapt (version 1.9.1) in order to trim adaptor sequences and low-quality bases, and remove trimmed sequences that were shorter than 80 nucleotides (nt) long (Martin, 2011). Quality base was set to 33 (default) and quality cutoff was set to 30 for the 5′ and 3′ ends. The first base of each sequence was also trimmed. The CD-HIT-DUP sequence clustering tool was then used to collapse reads with 99% global pairwise identity, leaving unique reads (Li and Godzik, 2006). Python-derived sequences were then filtered using the Bowtie2 alignment tool (version 2.2.5) (Langmead and Salzberg, 2012). First, a bowtie index was generated from the host genomic sequence [*Python bivittatus* (Burmese python) genome assembly (NC_021479.1)] and then sequences aligning with a –local mode alignment score greater than 60 were removed. SPAdes genome assembler (version 3.5.0) was used to generate contiguous sequences (contigs) (Bankevich et al., 2012). Then, to taxonomically categorize sequences, the NCBI nt database was queried with all contigs greater than 150 nt using the BLASTn alignment tool (version 2.2.30+) (Altschul et al., 1990; Camacho et al., 2009). Any hit with an expect value less than 10^{-8} was assigned taxonomically according to the sequence with the highest alignment score (Altschul et al., 1990; BLAST+ Command Line Applications User Manual, n.d.). Additionally, to attempt to categorize contigs that were too divergent to produce a high scoring nt-nt alignment, the NCBI nr database was queried using

Diamond (version 0.9.9.110) with an expect value of 0.001 (Buchfink et al., 2015). The same process was performed using all the reads that did not form contiguous sequences from SPAdes genomic assembly, except GSNAP alignment tool (version 2017-05-08) was used instead of BLASTn (Wu and Nacu, 2010). Lastly, a bowtie index was generated from ball python nidovirus 1 (NC_024709.1) and sequences aligning with a –local mode alignment score greater than 60 were evaluated in Geneious (version 9.0.5) for percent identity. The inoculum sequence was deposited in Genbank (accession MG752895) and raw sequence data was deposited in the NCBI Short Read Archive database (accession SRP118506).

3.13. Bacteriology

Oral swabs collected in agar medium (see “Experimental infection”) were submitted to the Colorado State University Veterinary Diagnostic Lab for aerobic bacterial culture.

4. Results

4.1. Antemortem clinical findings

Choanal, cloacal, and oroesophageal swabs tested negative for BPNV by qRT-PCR in all snakes prior to inoculation. Clinical signs in infected snakes (BP-A, B, and C) began at 4 weeks PI and progressed over time. Initial clinical signs were moderate reddening of the choanal and oral mucosa and excessive oral mucus secretion. With progression, oral reddening and mucus secretions became more severe resulting in excessive swallowing and ventral oral swelling. This was accompanied by small mucosal hemorrhages (petechiations), increased respiratory effort and rate, open-mouthed breathing, and anorexia by weeks 10–12 (Fig. 1).

4.2. Postmortem gross and histologic findings

BP-C displayed mild clinical signs (mucinous exudate in the oral cavity) at 5 weeks PI and was euthanized to assess lesions of early infection. Grossly, the oral mucosa was diffusely and mildly reddened with moderate mucinous secretions in the oral cavity and cranial esophagus. Histologically, there was moderate chronic-active mucinous rhinitis, stomatitis, glossitis, tracheitis, and cranial esophagitis with variable epithelial proliferation. Inflammatory infiltrates were mixed with moderate numbers of lymphocytes, plasma cells, heterophils and macrophages. There was mild faveolar pneumocyte hyperplasia regionally with the accumulation of luminal proteinaceous material. The caudal esophagus was normal.

BP-A was euthanized at 10 weeks PI and BP-B was euthanized at 12 weeks PI, both due to anorexia, intermittent increased respiratory effort and open-mouthed breathing, following IACUC protocol euthanasia criteria. Grossly, oral cavities of each snake were similar to BP-C but with significantly more mucinous exudate. BP-A also had a focal ulceration of the glottis, the caudal esophagus adjacent to the lungs was markedly dilated with air and mucus, and the cranial 1/3 of the lungs were wet and red (Fig. 2). BP-B lungs were slightly reddened and wet in the cranial portion but the caudal esophagus was grossly normal. Histologically, both snakes had similar but more severe lesions in the upper respiratory tract (URT) and cranial esophagus as compared to BP-C (Fig. 3A and B). Additionally, there were regions of erosion and ulceration in areas of inflammation as well as individual epithelial cell necrosis and regions of marked epithelial proliferation. The caudal esophagus of BP-A also had similar inflammatory infiltrates to that in the cranial esophagus but these were significantly milder. Lumina of the URT, cranial esophagus, central lumen of the lung, and faveoli contained mucus, necrotic debris, heterophils, hemorrhage, and occasional colonies of short Gram-negative bacterial rods. Both snakes (BP-A greater than BP-B) had a mild interstitial pneumonia of the cranial lung field with pneumocyte proliferation (Fig. 3C). Lesions were characterized by multifocal hyperplasia of respiratory epithelial cells lining the central lumen, hypertrophy and hyperplasia of faveolar pneumocytes (predominately in the luminal 1/3 of the faveoli), and expansion of the interstitium by edema and similar inflammatory cells to that in the URT.

Sham inoculated snakes (BP-D and E) did not show clinical signs nor have histologic lesions of the respiratory tract or esophagus (Fig. 3D-F). Both the infected and control snakes had moderate to severe lymphoplasmacytic and heterophilic, non-ulcerative colitis of unknown origin and mild lymphohistiocytic to granulomatous embolic hepatitis, which are considered unrelated to the clinical and histologic signs found only in the infected snakes. Gram, PAS, and Ziehl-Neelsen acid fast stains did not elucidate an infectious agent associated with these lesions. Remaining tissues were histologically normal (heart, kidneys, spleen, stomach, small intestine, pancreas, gall bladder, adrenal glands, gonads, brain, spinal cord, vertebral bone, bone marrow, skin, and skeletal muscle).

4.3. Western blot

DPHt cells inoculated with oroesophageal swabs from both infected and uninfected snakes were analyzed by western blot using anti-nucleocapsid protein polyclonal antisera to determine antibody specificity. This polyclonal antibody was designed in our laboratory and developed in rabbits, and this is the first demonstration of its specificity. The predicted length and molecular mass of the BPNV nucleocapsid protein is 152 aa and 16.7 kDa (GenBank: AIJ50569.1) and a protein of approximately this size was detected in BP-A, B, and C (infected) but not BP-D or E (control; Fig. 4).

Fig. 1. Antemortem findings. Clinical signs in infected snakes (BP-A, B, and C) began at 4 weeks PI and included moderate reddening of choanal and oral mucosa and abundant oral mucus secretion (A). This progressed to excessive swallowing, ventral oral swelling, mucosal petechiations, increased respiratory effort and rate, open-mouthed breathing (B), and anorexia by weeks 10–12. Control snakes were clinically normal throughout the experiment.

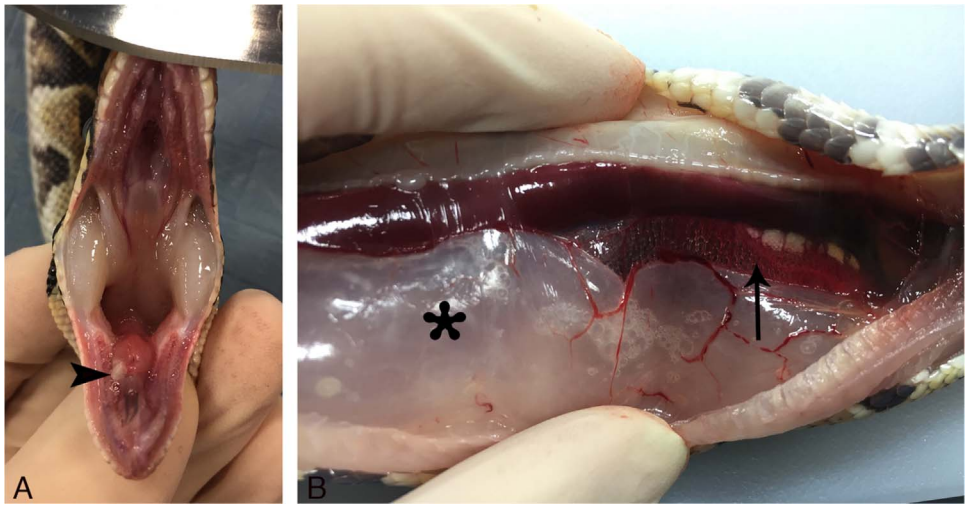

Fig. 2. Postmortem findings. Early lesions (BP-C) included diffuse reddening of the oral mucosa with moderate mucinous secretions in the oral cavity and cranial esophagus. Later lesions (BP-A and BP-B) included increased severity of early lesions with focal ulceration of the glottis in BP-A (A; arrowhead). The caudal esophagus adjacent to the lungs was markedly dilated with air and mucus (B; star), and the cranial 1/3 of the lungs were wet and red in BP-A (B; arrow). Control snakes were normal.

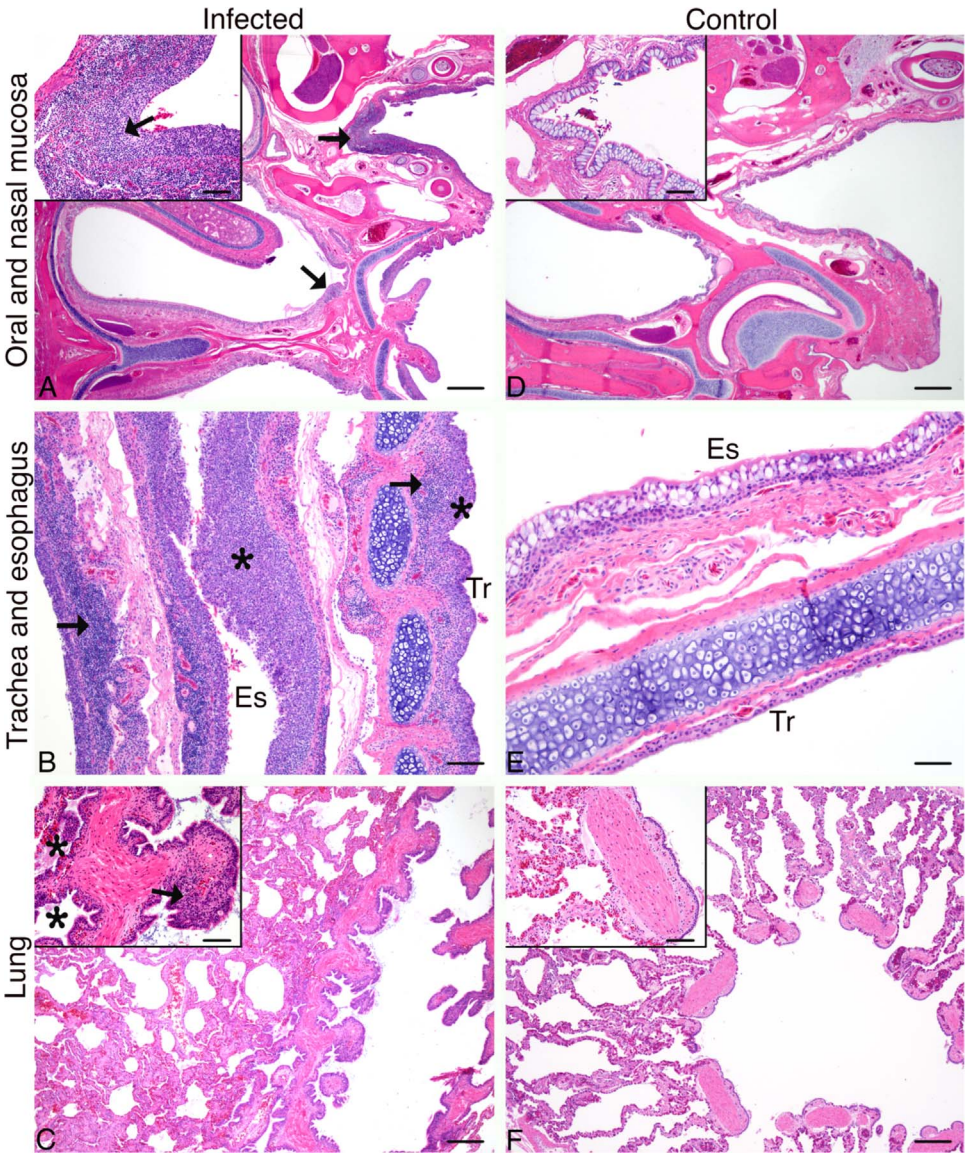

Fig. 3. Histopathology. Infected snakes had severe chronic-active mucinous rhinitis and stomatitis (A), tracheitis and esophagitis with epithelial proliferation (B), and interstitial proliferative pneumonia (C). Control snakes (D-F) were histologically normal. Arrows indicate inflammation; stars indicate epithelial proliferation. Hematoxylin and eosin. Boxes are represented in higher magnification in the insets (A, C, D, F). Scale bars: Inset scale 200 μm. (A) and (D) 1000 μm. (B) 200 μm. (E) 100 μm. (C) and (F) 500 μm. Esophagus (Es). Trachea (Tr).

4.4. Immunohistochemistry

Immunohistochemical staining of viral antigen (nucleocapsid protein) was present in all infected snakes within the epithelial surface of the oral mucosa, nasal mucosa, trachea, and esophagus (Fig. 5A-C). Immunopositive staining was detected in the cytoplasm of presumed

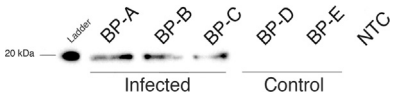

Fig. 4. Western blot of BPNV nucleoprotein. Viral nucleocapsid protein (approximately 16.7 kDa) was detected in DPHt cells inoculated with OES from BP-A, B, and C (infected) but not BP-D or E (control).

epithelial cells, predominately in regions of inflammation. Intact and degenerate cells containing viral antigen, or free viral antigen admixed with mucus was frequently present in the lumen of the URT and GI tract, or rarely faveoli (BP-A) (Fig. 5D). Within the caudal esophagus, stomach, small intestine, and colon viral antigen was restricted to the luminal contents and not detected in epithelial cells. However, regions of mucosal-associated lymphoid tissue of the caudal esophagus, small intestine, and colon contained low to moderate numbers of immunopositive cells suspected to be associated with M-cell-like uptake and sampling of the luminal contents (Fig. 6). Viral antigen was not detected in any other tissues in infected snakes (heart, kidneys, spleen, pancreas, gall bladder, adrenal glands, gonads, brain, spinal cord, vertebral bone, bone marrow, skin, and skeletal muscle). No viral antigen was detected in the control snakes.

4.5. Viral RNA detection

Viral RNA was detectable in oroesophageal, choanal, and cloacal swabs by qRT-PCR beginning at 1 week PI in all infected snakes, with an increase noted at 4 weeks PI in choanal and oroesophageal swab samples, coinciding with the onset of clinical signs. Levels of viral RNA increased steadily over the course of the experiment and reached levels exceeding 1000x more than the initial sampling time point (Fig. 7). Viral RNA was detected in multiple postmortem tissues from infected snakes, including trachea and esophagus, liver, kidney, heart, stomach, and feces, the lung of BP-A, and the small intestine and colon of BP-A and BP-C (Fig. 8). Respiratory and GI tract tissues and feces contained

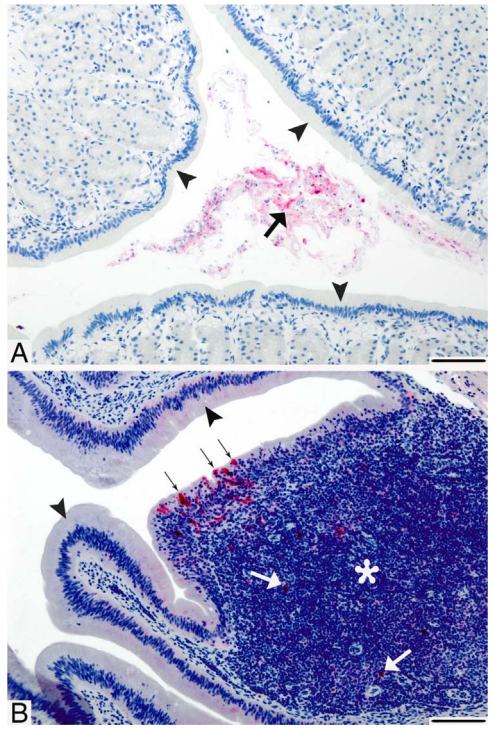

Fig. 6. Immunohistochemistry of the gastrointestinal tract. Representative images of the stomach (A) and small intestine (B) of infected snakes. Viral antigen (red staining) was detected in the lumen of the GI tract admixed with intact and degenerate cells and mucus (large black arrow). Epithelial cells (arrowheads) were immunonegative throughout the caudal esophagus and GI tract. However, viral antigen was detected in cells along the mucosal surface (small black arrows) overlying mucosal-associated lymphoid tissue (MALT; asterisk) of the esophagus, small intestine, and colon. Immunopositive cells extended into the center of MALT (white arrows). Primary antibody: polyclonal rabbit NdvNcAb. Counter stain: hematoxylin. Scale bars = 100 μm.

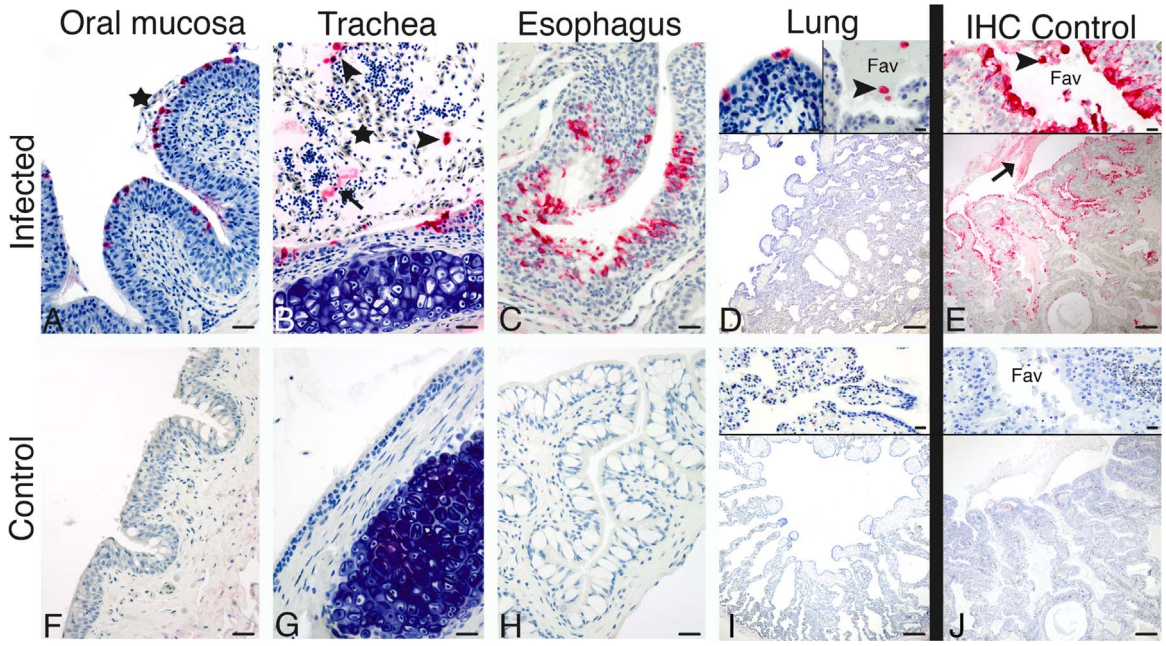

Fig. 5. Immunohistochemistry of the respiratory tract and cranial esophagus. Viral antigen (red staining) was prominent in the epithelial layer of the oral mucosa, trachea, and cranial esophagus of infected snakes (A-C). There were only rare positive cells within the pulmonary epithelium (D top left inset) and faveolar lumen (D top right inset) of one infected snake (BP-A), as compared with the positive IHC control from a nidovirus-positive green tree python that died of respiratory disease (E, lung). Intact and degenerate cells that contained viral antigen were also found in the lumen of these tissues (arrowheads) admixed with cell-free viral antigen in mucus (arrow) and hemorrhage (star). No viral antigen was detected in the control snakes (F-I). The IHC negative control (J) was the same lung tissue as that used for the positive control, but lacking primary antibody application. Fav, faveolar lumen; IHC, immunohistochemistry. Primary antibody: polyclonal rabbit NdvNcAb. Counter stain: hematoxylin. Scale bars: A-C and F-H = 50 μm; D-E and I-J lower = 500 μm, upper (inset) = 20 μm.

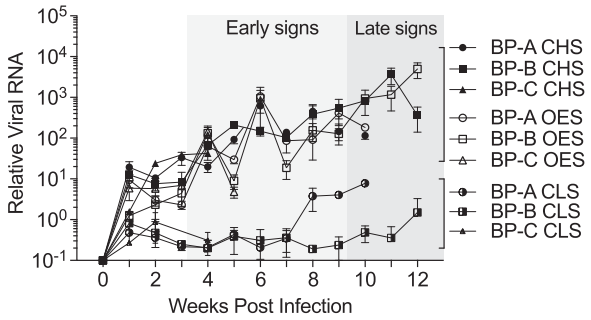

Fig. 7. Relative viral RNA in antemortem swabs. Total RNA was extracted from choanal (CHS), oroesophageal (OES), and cloacal (CLS) swabs and was analyzed by qRT-PCR using primers targeting BPNV RNA. Relative viral RNA was determined by comparison of each sample Ct to the sample with the highest Ct (lowest viral RNA) at the first collection time point following inoculation (BP-B OES week 1 PI). All samples were run in duplicate and error bars indicate standard deviations. Viral RNA was detectable beginning at 1 week PI in all swabs of the infected snakes, with an increase noted at 4 weeks PI, correlating with the initiation of clinical signs. Viral RNA continued to increase over the course of the experiment, consistent with amplification in the host. Early clinical signs included reddening of the oral mucosa and abundant oral mucus secretions. Late clinical signs included increased respiratory distress, open-mouthed breathing, and anorexia. Control snakes were negative throughout the experiment.

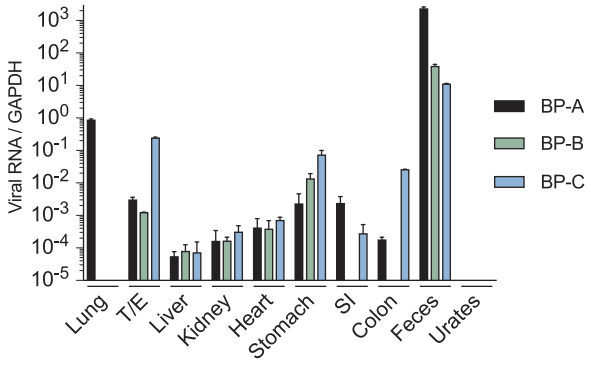

Fig. 8. Relative viral RNA in postmortem tissues. Total RNA was extracted from fresh tissues and analyzed by qRT-PCR. Relative viral RNA was determined by normalization of BPNV Ct to GAPDH (a cellular mRNA) Ct within each sample. All samples were run in duplicate and standard deviation is represented by error bars. Viral RNA was detected in nearly all tissues of infected snakes (BP-A, B, and C). Control snakes were negative in all tissues. T/E (trachea/esophagus); SI (small intestine).

the highest viral RNA per host mRNA (GAPDH), with remaining organs having detectable but lower viral RNA levels. Viral RNA was not detected in any swabs or tissues from control snakes.

4.6. Virus isolation

The presence of infectious virus in collected swabs, tissues, and excreta was evaluated by virus isolation in cell culture. Inoculation of DPHt cells with terminal oroesophageal swabs from infected snakes (BP-A, B, and C) resulted in viral replication, as determined by immunofluorescence using antibodies targeting the BPNV nucleocapsid protein, and cytopathic effects (Fig. 9). Speckled immunofluorescent staining was restricted to the cytoplasm of infected cells. Cytopathic effects included cell death and syncytial cell formation (Fig. 9 2DPI HM panel). Viral infection of cells was detected as early as 12 h PI with greater than 50% of cells infected by 2 days PI and significant cell death detected by day 4 PI. Plaque assay of the terminal oroesophageal swab from BP-A revealed a viral titer of 1.67×10^3 PFU/ml. Infectious virus was also isolated from feces of infected snakes, as determined by immunofluorescence of cell culture, but viral titers were not measured. Inoculation of DPHt cells with oral swabs and feces from control snakes (BP-D and E) did not produce detectable virus by immunofluorescence nor result in cytopathic effects. Virus isolation attempts with postmortem fresh lung samples from all snakes (infected and control) were negative.

4.7. Metagenomic sequencing

Metagenomic sequencing was used to validate the purity of the inoculum, to rule out other possible etiologic agents, and to evaluate genomic sequence of virus reisolated from infected snakes. The average number of read pairs per sample was 4.4×10^6. On average, 93%, 11%, and 3.6% of sequences remained following adaptor and quality filtering, collapsing to unique reads, and filtration of python derived sequences, respectively. Remaining sequences were compared against nucleotide and protein databases for taxonomic assessment. Sequences aligning to ball python nidovirus 1 (NCBI taxonomy ID: 1986118) and python nidovirus (NCBI taxonomy ID: 1526652) were detected in the lung and trachea/esophagus of BP-A, B, and C (infected snakes) and BPNV-148 inoculum. Nidovirus sequences were not detected in BP-D or E (control snakes). In addition to python nidovirus, BP-A lung had sequences aligning to *Pseudomonas* species. In all samples, *Python molurus* and *curtus* endogenous retrovirus-like sequences were detected. Other sequences aligning to organisms in the queried databases were predominately non-specific alignments due to low complexity or taxonomically ambiguous sequences that span multiple taxa. Other than *Pseudomonas* reads found in BP-A lung, no other sequences specifically aligning to known primary pathogenic or opportunistic infectious agents were identified. We analyzed the sequences generated through bowtie alignment of the BPNV inoculum and the viruses re-isolated from infected snakes. The sequence of the nidovirus in the inoculum was 96.2% identical to BPNV (NC_024709.1), and we obtained coverage across the complete genome. We did not obtain complete genome coverage for the recovered viruses, but the bowtie-mapped reads that did align to the BPNV sequence were 99.7–100% identical to the inoculum virus.

4.8. Bacteriology

Aerobic culture was performed on oral swabs from BP-A, B, D, and E. BP-A yielded heavy growth of *Pseudomonas aeruginosa* and *Stenotrophomonas maltophilia* and BP-B yielded moderate growth of *Bordatella* and *Pseudomonas* species. In the control snakes, BP-D yielded light growth of *Acinetobacter baumannii*, *Brevundimonas* species, *Delftia acidovorans*, and *Pseudomonas* species; BP-E yielded light growth of *Pseudomonas aeruginosa*.

5. Discussion

Novel nidoviruses were recently found in multiple python species with respiratory disease, but a causal relationship between infection and disease has not been established (Bodewes et al., 2014; Dervas et al., 2017; Marschang and Kolesnik, 2017; Stenglein et al., 2014; Uccellini et al., 2014). Through the use of experimental infections, our study is the first to fulfill Koch's postulates and demonstrate a causal relationship between python nidovirus infection and respiratory and esophageal disease in ball pythons. Our findings demonstrate that BPNV infection caused marked mucinous inflammation of the URT and cranial esophagus with progression towards proliferative interstitial pneumonia. These findings are consistent with previous reports of nidovirus infection in multiple python species (Bodewes et al., 2014; Dervas et al., 2017; Stenglein et al., 2014; Uccellini et al., 2014). In our study, the clinical hallmark of this disease was excessive mucous production in the oral cavity, which was accompanied histologically by marked inflammation and epithelial proliferation. Additionally, cranial esophagitis was a prominent lesion, similar to that in previous reports (Uccellini et al., 2014). Mucous production and esophagitis are not characteristic findings with other respiratory viruses in snakes and, therefore, may be useful clinical and histologic features for differential

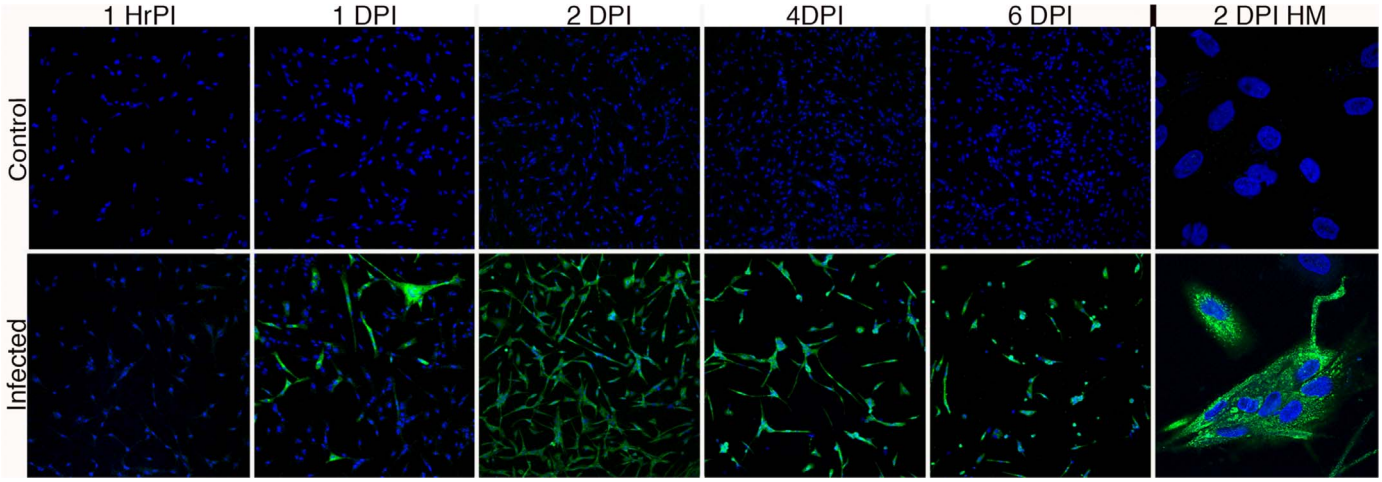

Fig. 9. Immunofluorescence of DPHt cells inoculated with infectious swabs and tissues. DPHt cells were inoculated with filtered terminal oroesophageal swabs (OES) and feces from infected snakes (BP-A OES represented in the bottom panel) resulting in viral infection, amplification, and cytopathic effects (syncytial formation and cell death). Inoculation with lung homogenate from infected snakes yielded negative results. Swabs and tissues from control snakes also yielded negative results. The top panel represents uninfected DPHt cells. HrPI (hours post infection); DPI (days post infection); HM (high magnification). Magnification is 100x in all images, except HM (high magnification) which is 1000x. Fluorescence is Hoescht 33342 (blue) for nuclear staining and Alexa 488 (green) for the BPNV nucleocapsid protein detection using NdvNcAb. All images include overlay of both fluorescence filters.

diagnosis of nidovirus infection in pythons. However, the overlap in clinical and histologic lesions with other viral agents (e.g. respiratory distress, anorexia, and proliferative pneumonia) could warrant the development of a multiplex PCR test to screen for multiple reptile respiratory viruses.

Viral antigen was detected in the mucosa of the oral and nasal cavity, trachea, and esophagus of all infected snakes, indicating a tropism for epithelial cells, especially ciliated cells of the respiratory tract and upper esophagus. Viral antigen was rarely detected in pulmonary epithelial cells, which may be due to the short time course of the experimental infections as discussed below. Viral antigen was not detected in the epithelium of the caudal esophagus or GI tract, but was present in the GI lumen by IHC and viral RNA was detected in these samples by qRT-PCR. This suggests that GI epithelium is not a site of viral replication, but the GI tract is a conduit for virus that is swallowed and passed in the feces. Additionally, viral antigen was detected in mucosal-associated lymphoid tissue of the caudal esophagus, small intestine, and colon. Sampling of the luminal contents by M-cell-like uptake could be a method for systemic spread, as indicated by viral RNA detection in non-respiratory/GI tissues.

Until recently, primary viral causes of pneumonia in pythons included paramyxovirus (ferlaviruses) and reovirus (Ariel, 2011; Jacobson, 2007a; Marschang, 2011). Other causes of proliferative pneumonia include chlamydophilosis, mycoplasmosis, chronic bacterial or parasitic infection, or toxin exposure (Bodetti et al., 2002; Jacobson, 2007b; Penner et al., 1997). Histopathology, bacterial culture, and next generation sequencing did not yield evidence of other primary infectious agents in the infected snakes or inoculum, consistent with BPNV as the principal cause of respiratory disease. The bacteria detected by oral aerobic culture and sequencing of the lung have been found as oral flora in clinically healthy snakes, (Blaylock, 2001; Goldstein et al., 1981; Plenz et al., 2015) but the presence of moderate to heavy growth in the infected snakes is suspected to be secondary to viral infection and disruption of physical or immune barriers. Secondary bacterial infections are a common sequelae to viral disease in all types of animals and humans and have been documented in previous cases of python nidoviral infection (Bodewes et al., 2014; Uccellini et al., 2014). The role of secondary infections and the progression of disease in pythons has yet to be determined and warrants further investigation.

In previous reports, the degree of pneumonia associated with nidovirus infection was more advanced at the time of death when compared to our study (Bodewes et al., 2014; Dervas et al., 2017; Stenglein et al., 2014; Uccellini et al., 2014). This is highlighted by our immunohistochemistry control (Fig. 5E) collected from a green tree python that had been nidovirus positive for over 6 months and eventually died of respiratory disease. Had we allowed for a longer time course of infection in this study, it is likely that the infected snakes would have progressed to more severe disease. Another possibility unexplored by this study, though suggested by other studies within our lab (unpublished data), is that some snakes clear nidovirus infection and recover.

Pythons have an overcapacity for oxygen consumption, and therefore rarely show clinical signs of respiratory disease until the oxygen exchange capacity is severely limited (Starck et al., 2015). A recent report in green tree pythons demonstrated infection of respiratory and faveolar epithelial cells to be associated with apoptosis, proliferation, and high numbers of serous/mucous granules within the cytoplasm (Dervas et al., 2017). Respiratory epithelial proliferation and mucus production were postulated to result in mechanical and physiologic inhibition of gas exchange within the lungs, resulting in death. Our study ended at 12 weeks PI based on euthanasia criteria, however the degree of respiratory effort was greater than would be expected for the mild pneumonia in the infected snakes. It is thought that the excessive production of mucus in the oral cavity and upper airway contributed to respiratory difficulty through obstruction of the airway and glottis. Therefore, the obstructive mechanical effects of mucus could also play a role in the upper respiratory tract by affecting overall air intake, in addition to the effects in the lung on direct oxygen exchange (Dervas et al., 2017).

Although the disease we observed closely resembles that seen in naturally infected snakes, there are several aspects of our study that may not have recapitulated natural infection. First, disease may be dose-dependent, and the 1.1×10^5 PFU administered may exceed a typical natural infectious dose. Second, the natural route(s) of transmission are unknown. Nidovirus RNA is detected in oral swabs (Marschang and Kolesnik, 2017) and respiratory/pulmonary epithelial cells of infected snakes (Dervas et al., 2017; Uccellini et al., 2014), indicating the oral cavity and respiratory tract as regions of viral replication and possible routes of exposure. We inoculated snakes in the oral cavity and upper trachea to mimic URT exposure and subsequently detected infectious virus in these regions indicating that virus is released in respiratory and oral secretions. Based on this finding, transmission may involve fomites or aerosolization. The presence of

infectious virus in the feces indicates that fecal-oral transmission is also possible.

Other factors, including husbandry, age, sex, and immune status could modulate disease progression. Care of the snakes in this study followed best practices for ball python husbandry. Snakes were housed separately with appropriate enclosures and climate control and handled minimally to limit stress. Although all snakes in this study were juvenile males (one was of undetermined sex), reports have documented nidovirus-associated respiratory disease in snakes of various sexes and ages (Dervas et al., 2017; Stenglein et al., 2014; Uccellini et al., 2014).

The python nidoviruses are part of an expanding clade of respiratory disease-associated toroviruses. A related virus has also been identified in wild shingleback lizards with respiratory disease (O'Dea et al., 2016). Clinical signs in lizards were similar to those observed in pythons, including excessive mucous in the oral cavity and anorexia. Additionally, a related nidovirus in cattle has been associated with severe tracheitis and pneumonia (Tokarz et al., 2015). The similar clinical findings suggest that viruses in this clade may share tissue tropism and pathogenic mechanisms. Related virus sequences have also been detected in snake-associated nematodes, though no information beyond sequence is available (Shi et al., 2016). That this clade includes viruses with reptilian, mammalian, and invertebrate hosts highlights its diversity, and emphasizes the need for further investigation into this expanding collection of potential pathogens.

Acknowledgements

The authors would like to thank the following groups and individuals: The histology laboratory at Colorado State University, Fort Collins Veterinary Diagnostic Laboratory for performing the histological and immunohistochemical procedures; Justin Lee and the CSU Next Generation Sequencing facility; the CSU Laboratory Animal Resources faculty and staff and Dr. Matt Johnston for help in snake handling and care; and Alora Lavoy and Lauren Kuechler for their contributions to this study.

Funding sources

Funding to develop and characterize the Diamond Python Heart cells used in this project was provided by the David R. Atkinson Center Academic Venture Fund at Cornell University (to J.S.L.P). Funding for experimental infections and subsequent disease characterization was provided by Colorado State University.

Conflict of interest

There is no conflict of interest.

References

Adams, M.J., Lefkowitz, E.J., King, A.M.Q., Harrach, B., Harrison, R.L., Knowles, N.J., Kropinski, A.M., Krupovic, M., Kuhn, J.H., Mushegian, A.R., Nibert, M., Sabanadzovic, S., Sanfaçon, H., Siddell, S.G., Simmonds, P., Varsani, A., Zerbini, F.M., Gorbalenya, A.E., Davison, A.J., 2017. Changes to taxonomy and the international code of virus classification and Nomenclature ratified by the international committee on taxonomy of viruses (2017). Arch. Virol. 162, 2505–2538. http://dx.doi.org/10.1007/s00705-017-3358-5.

Altschul, S.F., Gish, W., Miller, W., Myers, E.W., Lipman, D.J., 1990. Basic local alignment search tool. J. Mol. Biol. 215, 403–410. http://dx.doi.org/10.1016/S0022-2836(05)80360-2.

Ariel, E., 2011. Viruses in reptiles. Vet. Res. 42, 100. http://dx.doi.org/10.1186/1297-9716-42-100.

Bankevich, A., Nurk, S., Antipov, D., Gurevich, A.A., Dvorkin, M., Kulikov, A.S., Lesin, V.M., Nikolenko, S.I., Pham, S., Prjibelski, A.D., 2012. SPAdes: a new genome assembly algorithm and its applications to single-cell sequencing. J. Comput. Biol. 19, 455–477.

Batts, W.N., Goodwin, A.E., Winton, J.R., 2012. Genetic analysis of a novel nidovirus from fathead minnows. J. Gen. Virol. 93, 1247–1252. http://dx.doi.org/10.1099/vir.0.041210-0.

BLAST + Command Line Applications User Manual, n.d. [WWW Document]. URL ⟨http://www.ncbi.nlm.nih.gov/bookshelf/br.fcgi?Book=helpblast⟩.

Blaylock, R.S., 2001. Normal oral bacterial flora from some southern African snakes. Onderstepoort J. Vet. Res. 68, 175–182.

Bodetti, T.J., Jacobson, E., Wan, C., Hafner, L., Pospischil, A., Rose, K., Timms, P., 2002. Molecular evidence to support the expansion of the hostrange of Chlamydophila pneumoniae to include reptiles as well as humans, horses, koalas and amphibians. Syst. Appl. Microbiol. 25, 146–152. http://dx.doi.org/10.1078/0723-2020-00086.

Bodewes, R., Lempp, C., Schurch, A.C., Habierski, A., Hahn, K., Lamers, M., von Dornberg, K., Wohlsein, P., Drexler, J.F., Haagmans, B.L., Smits, S.L., Baumgartner, W., Osterhaus, A.D.M.E., 2014. Novel divergent nidovirus in a python with pneumonia. J. Gen. Virol. 95, 2480–2485. http://dx.doi.org/10.1099/vir.0.068700-0.

Buchfink, B., Xie, C., Huson, D.H., 2015. Fast and sensitive protein alignment using DIAMOND. Nat. Methods 12, 59–60. http://dx.doi.org/10.1038/nmeth.3176.

Camacho, C., Coulouris, G., Avagyan, V., Ma, N., Papadopoulos, J., Bealer, K., Madden, T.L., 2009. BLAST+: architecture and applications. BMC Bioinforma. 10, 421. http://dx.doi.org/10.1186/1471-2105-10-421.

De Groot, R., Cowley, J., Enjuanes, L., Faaberg, K., Perlman, S., Rottier, P., Snijder, E., Ziebuhr, J., Gorbalenya, A., 2012. Order - nidovirales. In: KIng, A.M., Adams, M.J., Carstens, E.B., Lefkowitz, E.J. (Eds.), Virus Taxonomy: Classification and Nomenclature of Viruses: Ninth Report of the International Committee on Taxonomy of Viruses. Elsevier, San Diego, pp. 784–794. http://dx.doi.org/10.1016/B978-0-12-384684-6.00066-5.

Dervas, E., Hepojoki, J., Laimbacher, A., Romero-Palomo, F., Jelinek, C., Keller, S., Smura, T., Hepojoki, S., Kipar, A., Hetzel, U., 2017. Nidovirus-associated Proliferative Pneumonia in the green tree Python (Morelia viridis). J. Virol. http://dx.doi.org/10.1128/JVI.00718-17.

Goldstein, E.J., Agyare, E.O., Vagvolgyi, A.E., Halpern, M., 1981. Aerobic bacterial oral flora of garter snakes: development of normal flora and pathogenic potential for snakes and humans. J. Clin. Microbiol. 13, 954–956.

Gonzalez, J.M., Gomez-Puertas, P., Cavanagh, D., Gorbalenya, A.E., Enjuanes, L., 2003. A comparative sequence analysis to revise the current taxonomy of the family Coronaviridae. Arch. Virol. 148, 2207–2235. http://dx.doi.org/10.1007/s00705-003-0162-1.

Graham, R.L., Donaldson, E.F., Baric, R.S., 2013. A decade after SARS: strategies for controlling emerging coronaviruses. Nat. Rev. Micro 11, 836–848.

Jacobson, E.R., 2007a. Infectious Diseases and Pathology of Reptiles. CRC Press (Chapter 9. Viruses and Viral Diseases of Reptiles).

Jacobson, E.R., 2007b. Infectious Diseases and Pathology of Reptiles. CRC Press (Chapter 5. Host response to infectious agents and identification of pathogens in tissue section).

Langmead, B., Salzberg, S.L., 2012. Fast gapped-read alignment with Bowtie 2. Nat. Methods 9, 357–359. http://dx.doi.org/10.1038/nmeth.1923.

Lauber, C., Ziebuhr, J., Junglen, S., Drosten, C., Zirkel, F., Nga, P.T., Morita, K., Snijder, E.J., Gorbalenya, A.E., 2012. Mesoniviridae: a proposed new family in the order Nidovirales formed by a single species of mosquito-borne viruses. Arch. Virol. 157, 1623–1628. http://dx.doi.org/10.1007/s00705-012-1295-x.

Li, W., Godzik, A., 2006. Cd-hit: a fast program for clustering and comparing large sets of protein or nucleotide sequences. Bioinformatics 22, 1658–1659. http://dx.doi.org/10.1093/bioinformatics/btl158.

Marschang, R.E., 2011. Viruses infecting reptiles. Viruses 3, 2087–2126. http://dx.doi.org/10.3390/v3112087.

Marschang, R.E., Kolesnik, E., 2017. Detection of nidoviruses in live pythons and boas. Tierarztl. Prax. Ausg. K. Klient. Heimtiere 45, 22–26. http://dx.doi.org/10.15654/TPK-151067.

Martin, M., 2011. Cutadapt removes adapter sequences from high-throughput sequencing reads. EMBnet. J. 17.

Masters, P.S., Perlman, S., 2013. Coronaviridae. In: Knipe, D.M., Howley, P.M. (Eds.), Fields Virology. Lippincott Williams & Wilkins, pp. 825–858.

Nga, P.T., Parquet, M., del, C., Lauber, C., Parida, M., Nabeshima, T., Yu, F., Thuy, N.T., Inoue, S., Ito, T., Okamoto, K., Ichinose, A., Snijder, E.J., Morita, K., Gorbalenya, A.E., 2011. Discovery of the first insect nidovirus, a missing evolutionary link in the emergence of the largest RNA virus genomes. PLoS Pathog. 7, e1002215. http://dx.doi.org/10.1371/journal.ppat.1002215.

O'Dea, M.A., Jackson, B., Jackson, C., Xavier, P., Warren, K., 2016. Discovery and partial genomic characterisation of a novel nidovirus associated with respiratory disease in wild Shingleback Lizards (Tiliqua rugosa). PLoS One 11, e0165209. http://dx.doi.org/10.1371/journal.pone.0165209.

Penner, J.D., Jacobson, E.R., Brown, D.R., Adams, H.P., Besch-Williford, C.L., 1997. A novel Mycoplasma sp. associated with proliferative tracheitis and pneumonia in a Burmese python (Python molurus bivittatus). J. Comp. Pathol. 117, 283–288.

Plenz, B., Schmidt, V., Grosse-Herrenthey, A., Kruger, M., Pees, M., 2015. Characterisation of the aerobic bacterial flora of boid snakes: application of. Vet. Rec. 176, 285. http://dx.doi.org/10.1136/vr.102580.

Pradesh, U., Chikitsa, P.D.D.U.P., Vishwa, V., Dhcirnci, C., Izcitncigcir, B., 2014. Toroviruses affecting animals and humans: a review. Asian J. Anim. Vet. Adv. 9, 190–201.

Runckel, C., Flenniken, M.L., Engel, J.C., Ruby, J.G., Ganem, D., Andino, R., DeRisi, J.L., 2011. Temporal analysis of the honey bee microbiome reveals four novel viruses and seasonal prevalence of known viruses, Nosema, and Crithidia. PLoS One 6, e20656. http://dx.doi.org/10.1371/journal.pone.0020656.

Schutze, H., Ulferts, R., Schelle, B., Bayer, S., Granzow, H., Hoffmann, B., Mettenleiter, T.C., Ziebuhr, J., 2006. Characterization of White bream virus reveals a novel genetic cluster of nidoviruses. J. Virol. 80, 11598–11609. http://dx.doi.org/10.1128/JVI.01758-06.

Shi, M., Lin, X.-D., Tian, J.-H., Chen, L.-J., Chen, X., Li, C.-X., Qin, X.-C., Li, J., Cao, J.-P., Eden, J.-S., Buchmann, J., Wang, W., Xu, J., Holmes, E.C., Zhang, Y.-Z., 2016.

Redefining the invertebrate RNA virosphere. Nature. http://dx.doi.org/10.1038/nature20167.

Snijder, E.J., Kikkert, M., 2013a. Arteriviruses. In: Knipe, D.M., Howley, P.M. (Eds.), Fields Virology. Lippincott Williams & Wilkins, pp. 859–879.

Snijder, E.J., Kikkert, M., Fang, Y., 2013b. Arterivirus molecular biology and pathogenesis. J. Gen. Virol. 94, 2141–2163.

Starck, J.M., Weimer, I., Aupperle, H., Muller, K., Marschang, R.E., Kiefer, I., Pees, M., 2015. Morphological pulmonary diffusion capacity for oxygen of Burmese Pythons (Python molurus): a comparison of animals in healthy condition and with different pulmonary infections. J. Comp. Pathol. 153, 333–351. http://dx.doi.org/10.1016/j.jcpa.2015.07.004.

Stenglein, M.D., Jacobson, E.R., Wozniak, E.J., Wellehan, J.F.X., Kincaid, A., Gordon, M., Porter, B.F., Baumgartner, W., Stahl, S., Kelley, K., Towner, J.S., DeRisi, J.L., 2014. Ball python nidovirus: a candidate etiologic agent for severe respiratory disease in Python regius. mBio 5, e01484–1414. http://dx.doi.org/10.1128/mBio.01484-14.

Stenglein, M.D., Jacobson, E.R., Chang, L.-W., Sanders, C., Hawkins, M.G., Guzman, D.S.-M., Drazenovich, T., Dunker, F., Kamaka, E.K., Fisher, D., Reavill, D.R., Meola, L.F., Levens, G., DeRisi, J.L., 2015. Widespread recombination, reassortment, and transmission of unbalanced compound viral genotypes in natural arenavirus infections. PLoS Pathog. 11, e1004900. http://dx.doi.org/10.1371/journal.ppat.1004900.

Stenglein, M.D., Sanchez-Migallon Guzman, D., Garcia, V.E., Layton, M.L., Hoon-Hanks, L.L., Boback, S.M., Keel, M.K., Drazenovich, T., Hawkins, M.G., DeRisi, J.L., 2017. Differential disease susceptibilities in experimentally REptarenavirus-infected Boa Constrictors and Ball Pythons. J. Virol. 91. http://dx.doi.org/10.1128/JVI.00451-17.

Tokarz, R., Sameroff, S., Hesse, R.A., Hause, B.M., Desai, A., Jain, K., Lipkin, W.I., 2015. Discovery of a novel nidovirus in cattle with respiratory disease. J. Gen. Virol. 96, 2188–2193. http://dx.doi.org/10.1099/vir.0.000166.

Uccellini, L., Ossiboff, R.J., de Matos, R.E.C., Morrisey, J.K., Petrosov, A., Navarrete-Macias, I., Jain, K., Hicks, A.L., Buckles, E.L., Tokarz, R., McAloose, D., Lipkin, W.I., 2014. Identification of a novel nidovirus in an outbreak of fatal respiratory disease in ball pythons (Python regius). Virol. J. 11, 144. http://dx.doi.org/10.1186/1743-422X-11-144.

Wu, T.D., Nacu, S., 2010. Fast and SNP-tolerant detection of complex variants and splicing in short reads. Bioinformatics 26, 873–881. http://dx.doi.org/10.1093/bioinformatics/btq057.